Article

Not peer-reviewed version

Genome-Wide Analysis of Ammonium Transporter Genes in Flowering Chinese Cabbage and Functional Insights into BcAMT1.1 Under Low Nitrogen Conditions

Yunna Zhu *, Lihua Zhong, Qiiuxiang Zhong, Xinmin Huang, Ali Anwar, Wei Su, Riyuan Chen *, Shiwei Song *

Posted Date: 14 November 2025

doi: 10.20944/preprints202511.1072.v1

Keywords: ammonium transporter; flowering Chinese cabbage; low nitrogen conditions; genomewide analysis

Article

Genome-Wide Analysis of Ammonium Transporter Genes in Flowering Chinese Cabbage and Functional Insights into BcAMT1.1 Under Low Nitrogen Conditions

Yunna Zhu [1,2,†], Lihua Zhong [1,3,†], Qiuxiang Zhong [1], Xinmin Huang [1,4], Ali Anwar [1], Wei Su [1], Riyuan Chen [1,*] and Shiwei Song [1,*]

[1] College of Horticulture, South China Agricultural University, Guangzhou, 510642, China
[2] College of Biology and Agriculture, Shaoguan University, Shaoguan, 512005, China
[3] College of Agriculture and Food Engineering, Baise University, Baise, 533000, China
[4] Guangdong Provincial Key Laboratory for Green Agricultural Production and Intelligent Equipment/College of Biology and Food Engineering, Guangdong University of Petrochemical Technology, Maoming 525000, China
* Correspondence: rychen@scau.edu.cn (R.C.); swsong@scau.edu.cn (S.S.); Tel.: +86-20-38294595 (R.C.); +86-20-85280228 (S.S.)
† These authors contributed equally to this work.

Abstract

As a primary macronutrient, nitrogen is integral to plant growth and developmental regulation; ammonium transporters (AMTs) mediate its absorption and involvement in nitrogen metabolism. In this study, nine *BcAMT* genes were identified from flowering Chinese cabbage (*Brassica campestris*), which were systematically categorized into two subfamilies. Their evolutionary relationships, conserved motifs, chromosomal distribution, cis-regulatory elements, and expression profiling were systematically characterized. RNA-sequencing and RT-PCR analyses demonstrated that *BcAMT1.1* was abundantly expressed in roots, leaves, and stems of flowering Chinese cabbage, and was markedly up-regulated under nitrogen deficiency or low-nitrogen conditions. Subcellular location using GFP-fusion demonstrated that BcAMT1.1 localized to the plasma membrane. Functional assays through heterologous expression in the yeast mutant strain 31019b and transgenic *Arabidopsis* validated that BcAMT1.1 acted as a functional ammonium transporter. Compared with wildtype, overexpressing *BcAMT1.1* promoted seedling growth, enhanced NH_4^+ influxes and NO_3^- effluxes under low nitrogen conditions, and significantly increased the transcription levels of key nitrogen assimilation genes (i.e., *AtGLN1.1*, *AtGLN2*, *AtGDH2*). Collectively, our findings enhance the fundamental understanding of *BcAMT* gene functions, and highlighting of BcAMT1.1 as a crucial component in nitrogen uptake and assimilation under low nitrogen conditions, and providing valuable genetic resources for improving nitrogen efficiency in vegetable crops.

Keywords: ammonium transporter; flowering Chinese cabbage; low nitrogen conditions; genome-wide analysis

1. Introduction

Nitrogen, as a critical macronutrient, is indispensable for plant physiological functioning and is responsible for up to 50% of biomass accumulation [1]. Due to its significant added value, nitrogen fertilizers are often applied in excess of actual crop demands as a low-cost insurance against potential yield losses [2,3]. In vegetable crop production, over-application, combined with low nitrogen recovery and intensive irrigation, markedly reduces nitrogen use efficiency (NUE) and generates dual

 doi:10.20944/preprints202511.1072.v1

environmental and health risks, including water pollution, greenhouse gas emissions, and excessive nitrate accumulation in edible plant organs, particularly in leafy vegetables [2]. Thus, improving NUE is essential for sustainable agricultural production and relies on a thorough understanding of the mechanisms governing nitrogen absorption, transport, and metabolism.

Ammonium (NH_4^+) and nitrate (NO_3^-) are the main inorganic nitrogen sources utilized by plants [4]. In soils, NH_4^+ concentrations (20 to 200 μmol·L^{-1}) are lower than those of NO_3^- (100 μmol·L^{-1} to 70 mmol·L^{-1}) [5,6]. Although NO_3^- is generally the predominant nitrogen form for most plants, NH_4^+ may be preferred under nitrogen deficiency or elevated atmosphere carbon dioxide, because it requires less energy for assimilation via the glutamine synthetase/NADH-dependent glutamate synthase (GS/GOGAT) pathway [7,8]. Nevertheless, excessive NH_4^+ can be toxic to plants [6,9]. Therefore, NH_4^+ uptake and transportation require to be tightly regulated. NH_4^+ uptake in plants is mediated by two distinct systems: the high-affinity transport system (HATS) and the low-affinity transport system (LATS). HATS operates predominantly at low NH_4^+ levels, ensuring efficient NH_4^+ absorption, whereas LATS becomes more active at higher NH_4^+ concentrations [10,11]. NH_4^+ uptake at low NH_4^+ level (< 1 mmol·L^{-1}) is predominantly regulated by HATS [12]. Ammonium transporters (AMTs), members of AMT/methylammonium permease (MEP)/rhesus (Rh) protein family, are key mediators of NH_4^+ uptake and transport in plants [11,13]. AMT proteins, mainly found in plants, are grouped into two major subfamilies: the AMT1 subfamily, comprising only AMT1 cluster, and the AMT2 subfamily, including AMT2, AMT3, and AMT4 clusters [14]. The AMT2 shows high homology to yeast MEP and *Escherichia coli* AmtB, but less homologous to AMT1 proteins [15].

Following the identification of the first *AMT* in *Arabidopsis* [16], the members of AMT have subsequently been reported in various species, including rice[17,18], rapeseed [19], soybean [20], and tobacco [21]. In *Arabidopsis*, six AMTs have been isolated and characterized, including five members of AMT1 subfamily and a single AMT2 isoform [22,23]. Among them, *AtAMT1.1* ~ *AtAMT1.3*, and *AtAMT1.5* are primarily expressed in roots and strongly induced by nitrogen deficiency or low nitrogen conditions, with AtAMT1.1 ~ AtAMT1.3 account for nearly 90% of high-affinity NH_4^+ absorption [22]. AtAMT1.4 is a pollen-specific AMT member and mediates NH_4^+ absorption in pollen [24]. In rice, 12 AMTs are isolated, OsAMT1.1 ~ OsAMT1.3 account for up to 95% of high-affinity NH_4^+ uptake [18]; the knockout of *OsAMT1.1* reduces NH_4^+ uptake by 25~30% [25]. In rapeseed, 20 *BnaAMT* genes are identified, with 14 members from the AMT1 subfamily and six from the AMT2 subfamily, most of which are highly responsive to external nitrogen conditions [19].

Flowering Chinese cabbage (*Brassica campestris* L. ssp. *chinensis* var. *utilis* Tsen et Lee), is typical stalk vegetable originated from South China, possessing significant health and economic values [26,27]. Flowering Chinese cabbage is now cultivated globally, particularly in Asian countries [26,28], and requires substantial nitrogen input to achieve optimal yield; hence, excessive NO_3^- often accumulates in edible organs, especially in stalks, posing potential health risks [29,30]. Understanding the molecular mechanism of nitrogen uptake and transportation in flowering Chinese cabbage could inform strategies to optimize fertilization practices and improve NUE. Here, we present a genome-wide survey and detailed analysis of the *AMT* gene family in flowering Chinese cabbage. We examined their phylogenetic relationships, conserved motifs, gene structures, chromosomal localization, syntenic patterns, cis-regulatory elements, and expression patterns. Among these, *BcAMT1.1* showed strong transcriptional induction under low nitrogen concentration. Functional assays of *BcAMT1.1* in yeast mutant strain 31019b confirmed its functional NH_4^+ transport activity, and overexpression in *Arabidopsis* enhanced seedling growth, NH_4^+ uptake, and nitrogen assimilation-related genes transcription under low-nitrogen conditions. This study underscores the pivotal role of AMTs in plant growth and nitrogen metabolism, with BcAMT1.1 being critical for nitrogen acquisition and assimilation under low nitrogen conditions, and provide genetic resources for improving NUE in vegetable crops.

2. Results

 doi:10.20944/preprints202511.1072.v1

2.1. Identification and Chromosomal Localization of BcAMT Gene Family in Flowering Chinese Cabbage

Potential AMT members were identified from flowering Chinese cabbage genome through BLASTP searches using *Arabidopsis* AMT protein sequences, obtained from the BRAD database. Candidate sequences were confirmed to contain the Pfam domain of ammonium transporter family (PF00909). In total, nine BcAMT members were identified and designated BcAMT1.1 to BcAMT2.1-like, according to their homology with *Arabidopsis* AMTs. The physiochemical properties of BcAMTs were assessed using the EXPASY ProtParam, including molecular weight (MW), isoelectric point (pI), amino acids number, and grand average of hydropathy (GRAVY). Amino acid number ranged from 476 (BcAMT1.3-like) to 512 aa (BcAMT1.2), with the predicted MW ranging from 50.79 (BcAMT1.3-like) to 54.88 kDa (BcAMT1.2). The pI values varied from 5.45 (BcAMT1.4-like) to 7.73 (BcAMT1.2), indicating that most members were weakly acidic. All instability indices were below 40, and the GRAVY value was higher than zero, suggesting that these BcAMT proteins were stable and hydrophobic. Subcellar localization analysis revealed that all BcAMT proteins are positioned in the plasma membrane, with 9 to 11 transmembrane domains (Table 1), consistent with membrane-associated transport functions of AMT. Chromosomal mapping showed that nine *BcAMTs* were dispersed across six chromosomes (Chr) of flowering Chinese cabbage genome (Table 1; Figure 1), *BcAMT1.3-like* and *BcAMT1.4* were located on Chr1; *BcAMT1.4-like* and *BcAMT1.5* on Chr3; *BcAMT1.1* and *BcAMT2.1* on Chr5; *BcAMT2.1-like*, *BcAMT1.3*, and *BcAMT1.2* on Chr4, Chr7, and Chr9.

Table 1. Characteristics of *BcAMT* gene family members in flowering Chinese cabbage.

Gene ID	Gene Name	Chr	Start	End	MW (kDa)	pI	AA (aa)	Instability index	GRAVY	TM	Subcellular localization	Category
Bra_cxA05g029310.1	*BcAMT1.1*	A05	9051433	9052957	53.62	7.13	503	25.33	0.38	9	Cell membrane	AMT1
Bra_cxA09g068650.1	*BcAMT1.2*	A09	1262097	1263778	54.88	7.73	512	24.10	0.35	10	Cell membrane	AMT1
Bra_cxA07g035530.1	*BcAMT1.3*	A07	8638823	8640466	54.11	6.74	504	28.46	0.35	9	Cell membrane	AMT1
Bra_cxA01g016480.1	*BcAMT1.3-like*	A01	20920458	20926484	50.79	5.87	476	26.46	0.39	10	Cell membrane	AMT1
Bra_cxA01g038520.1	*BcAMT1.4*	A01	4314030	4315548	53.66	5.7	501	26.06	0.43	10	Cell membrane	AMT1
Bra_cxA03g011620.1	*BcAMT1.4-like*	A03	28109231	28110768	54.41	5.45	509	27.01	0.45	10	Cell membrane	AMT1
Bra_cxA03g025790.1	*BcAMT1.5*	A03	20119522	20121038	53.17	5.96	500	25.32	0.43	10	Cell membrane	AMT1
Bra_cxA05g037880.1	*BcAMT2.1*	A05	3982245	3986822	52.63	6.32	489	28.53	0.45	11	Cell membrane	AMT2
Bra_cxA04g005660.1	*BcAMT2.1-like*	A04	23713465	23716475	52.52	7.28	488	25.86	0.45	11	Cell membrane	AMT2

AA: amino acids; Chr: chromosome; GRAVY: grand average of hydropathy; MW: molecular weight; pI: isoelectric point; TM: transmembrane.

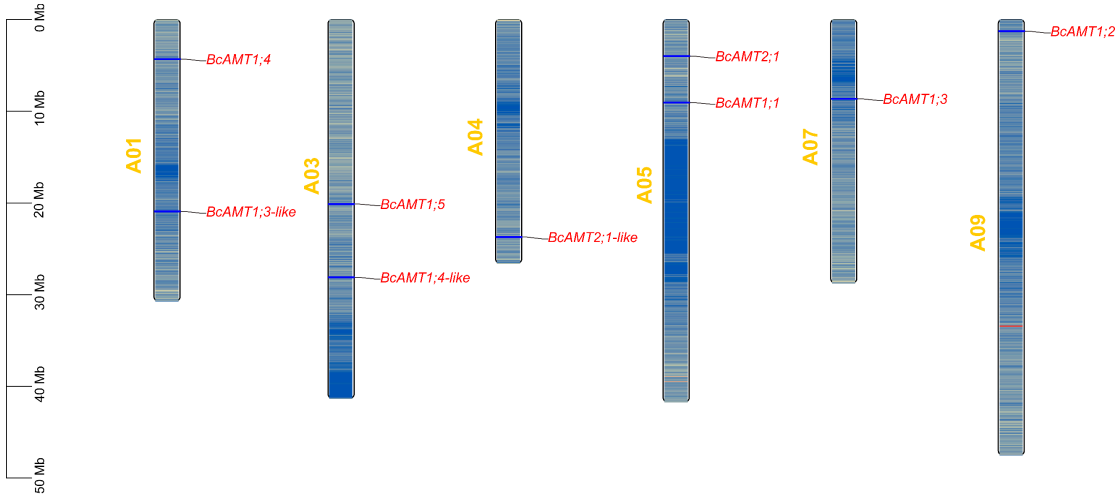

 doi:10.20944/preprints202511.1072.v1

Figure 1. Chromosomal location of *BcAMT* genes in flowering Chinese cabbage. Bars represent individual chromosomes, with color gradients indicating gene density along each chromosome. Physical gene positions are marked, and scale bar denotes relative chromosome length in megabase (Mb) units.

2.2. Phylogenetic Tree and Conserved Domains Analyses of BcAMT Gene Family

To evaluate the evolutionary relationships of AMT proteins, a maximum likelihood (ML) phylogenetic tree was generated in MEGA 7.0, incorporating AMTs from flowering Chinese cabbage, *Arabidopsis thaliana*, *Brassica napus*, *Solanum lycopersicum*, *Nicotiana tabacum*, *Oryza sativa*, and *Populus trichocarpa* (Table S1). The phylogenetic tree resolved into two dominant clades (Figure 2A): seven BcAMTs grouped within the AMT1 subfamily and two within AMT2. Both two AMT2 members were found in Cluster II, and no flowering Chinese cabbage or other Cruciferae AMTs were placed in cluster III or IV. Homology analysis showed that BcAMTs shared high homology with *Arabidopsis* AtAMTs and rapeseed BnaAMTs, with orthologous counterparts in flowering Chinese cabbage (Figure 2A). Furthermore, several paralogous gene pairs were identified, including *BcAMT1.3*/*BcAMT1.3-like*, *BcAMT1.4*/ *BcAMT1.4-like*, and *BcAMT2.1*/*BcAMT2.1-like*, each gene pair clustering with the corresponding AMT members in *Arabidopsis* and rapeseed, suggesting possible functional redundancy. Signature motif analysis, performed in Jalview v2.11.2.7, revealed that all AMT1 subfamily members shared the conserved sequence "DFAGSGVVHMVGGIAGLWGALIEGPR", except BnaAMT1.3c in rapeseed; while all AMT2 members universally contained the conserved sequence "DYSGGYIHLSSGVAGFTAAYW WGPR", except OsAMT4.1 in *O. sativa* (Figure 2B, C). The signatures motifs strongly support the phylogenetic classification.

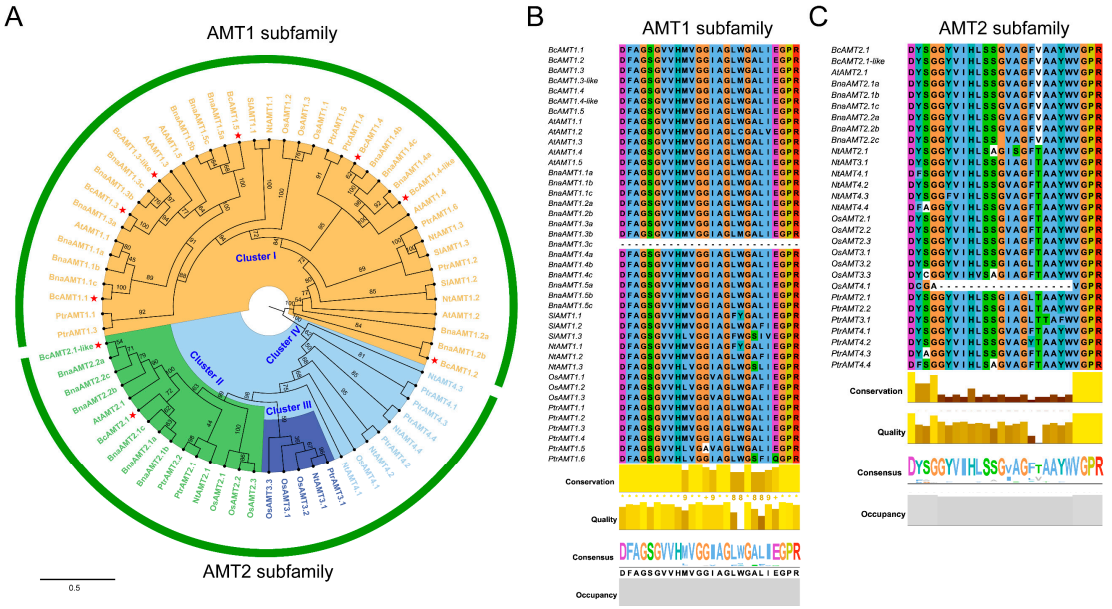

Figure 2. Phylogenetic relationships and conserved signature sequences of AMTs. (**A**) Phylogenetic tree of AMTs was constructed using MEGA 7.0, with bootstrap values calculated from 1000 replications. *At*: *Arabidopsis thaliana*; *Sl*: *Solanum lycopersicum*; *Nt*: *Nicotiana tabacum*; *Os*: *Oryza sativa*; *Ptr*: *Populus trichocarpa*; *Bn*: *Brassica napus*; *Bc*: *Brassica campestris*. (**B**) Conserved signature sequences of the AMT1 subfamily. (**C**) Conserved signature sequences of the AMT2 subfamily.

2.3. Conserved Motifs and Gene Structure of BcAMT Gene Family

Motif composition and gene structure were analyzed in relation to evolutionary classification. Among all BcAMT members, ten consensus motifs were identified, which were present in seven BcAMT1 subfamily, whereas BcAMT2.1 and BcAMT2.1-like contained seven and six motifs,

 doi:10.20944/preprints202511.1072.v1

respectively. Six conversed motifs (motif 3, 4, 5, 6, 8 and 10) were conserved across all BcAMT members (Figure 3A). Domain prediction showed that all BcAMT proteins contained the characteristic ammonium transporter domain (amt) (Figure 3B). Gene structure analysis revealed marked differences between subfamilies: *BcAMT2* members harbored four introns, while most *BcAMT1* members were intronless except *BcAMT1.2* and *BcAMT1.3-like* (Figure 3C). These differences in gene structure may underpin functional divergence between BcAMT1 and BcAMT2 subfamilies.

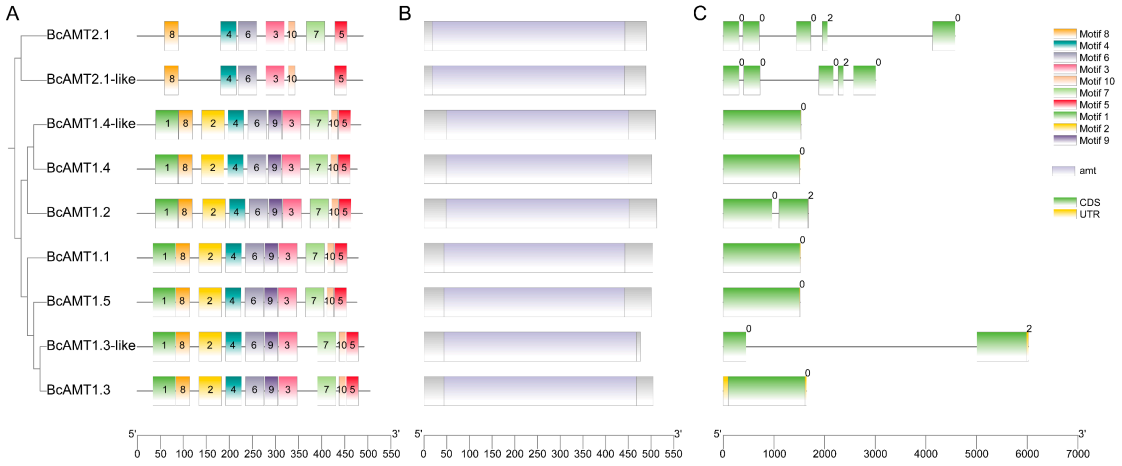

Figure 3. Conserved motif composition, domain architecture, and gene structure of BcAMTs. (**A**) Phylogenetic tree and motifs distribution. (**B**) Conserved domain analysis. (**C**) Gene structure analysis.

2.4. Gene Duplication and Synteny Analyses of the BcAMT Gene Family

To understand the evolutionary expansion of the *BcAMT* gene family, genome-wide collinearity analysis was performed using the MCScan X module in TBtools-II. Five segmentally gene pairs were identified: *BcAMT1.3*/*BcAMT1.3-like*, *BcAMT1.4*/*BcAMT1.4-like*, *BcAMT1.3*/ *BcAMT1.5*, *BcAMT1.5*/*BcAMT1.3-like*, and *BcAMT2.1*/*BcAMT2.1-like* (Figure 4A; Table 2). The segmental duplications likely played a vital role in the expansion of BcAMT family in flowering Chinese cabbage. Based on the rates of synonymous (Ks) and nonsynonymous (Ka) substitution, and assuming a neutral divergence rate of 1.5×10^{-8} substitutions per site per year, divergence times of these paralogous pairs were estimated to range from 10.5503 to 24.7684 million years ago (MYA), averaging ~16.9060 MYA (Table 2). The ratios of Ka/Ks ranged from 0.0962 and 0.1383, remaining well below 1.0, implying that these duplicates of *BcAMTs* have experienced intense purifying selection during evolution.

Comparative synteny mapping revealed the extensive collinear relationships between *BcAMT* genes and *AMT*s in *Arabidopsis* and *B. napus*, while no syntenic associations with *O. sativa*. Seven *BcAMT* genes exhibited syntenic correlation with *Arabidopsis AMT*s and nine with *B. napus AMTs* (Figure 4B; Table S2). Specific relationships included *BcAMT1.3*, *BcAMT1.3-like*, *BcAMT1.5* with *AtAMT1.1* and *AtAMT1.5*; *BcAMT1.4* and *BcAMT1.4-like* with *AtAMT1.4*; *BcAMT2.1* and *BcAMT2.1-like* with *AtAMT2.1* (Figure 4; Table S2). In *B. napus*, there were many syntenic relationships, *BcAMT1.1* with *BnaAMT1.1b*, *BcAMT1.2* with *BnaAMT1.2a* and *BnaAMT1.2b*; *BcAMT1.3*, *BcAMT1.3-like* and *BcAMT1.5* with *BnaAMT1.3a* and *BnaAMT1.5a*; *BcAMT1.4* and *BcAMT1.4-like* with *BnaAMT1.4a*, *BnaAMT1.4b* and *BnaAMT1.4c*; *BcAMT2.1* and *BcAMT2.1-like* with *BnaAMT2.1a*, *BnaAMT2.1c*, and *BnaAMT2.2c* (Figure 4; Table S2). These syntenic relationships highlight a conserved genomic context of *BcAMT*s within *Brassica* species and the divergence from monocot *AMTs*.

 doi:10.20944/preprints202511.1072.v1

Table 2. Divergence time estimation for paralogous gene pairs of *BcAMTs*.

Seq_1	Seq_2	Identity (%)	Ka	Ks	Ka/Ks	T/ (MYA)
BcAMT1.3	BcAMT1.3-like	87.30	0.0394	0.4100	0.0962	13.6678
BcAMT1.5	BcAMT1.3	84.33	0.0903	0.6636	0.1360	22.1207
BcAMT1.5	BcAMT1.3-like	81.04	0.0782	0.7431	0.1053	24.7684
BcAMT1.4	BcAMT1.4-like	90.57	0.0454	0.4027	0.1129	13.4226
BcAMT2.1	BcAMT2.1-like	92.84	0.0438	0.3165	0.1383	10.5503

Ks: synonymous substitution rate, Ka: nonsynonymous substitution rate, T: divergence time.

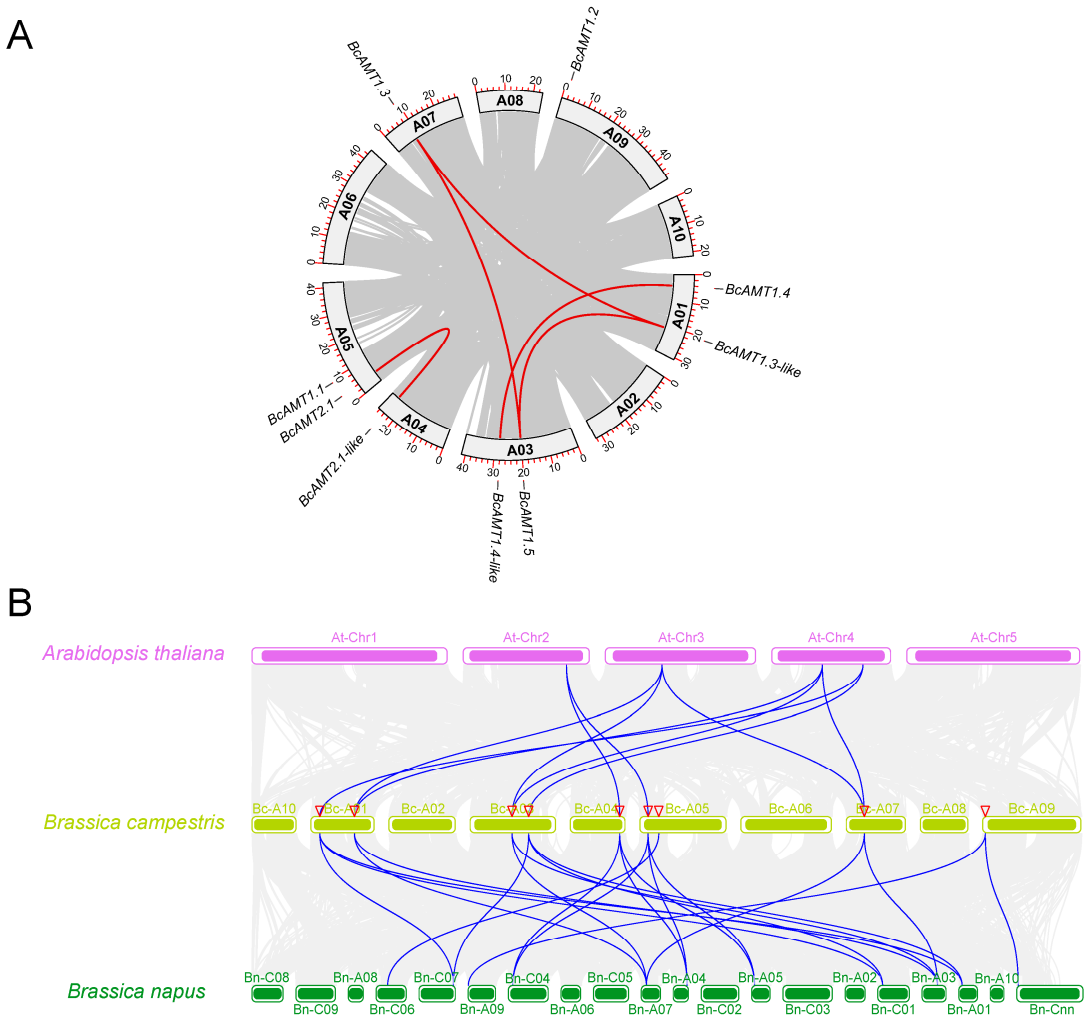

Figure 4. Collinearity patterns of the *AMTs* gene family. (**A**) Collinearity relationships of *AMT*s in flowering Chinese cabbage. (**B**) Comparative synteny among *A. thaliana*, *B. napus*, and flowering Chinese cabbage.

2.5. Analysis of Cis-Acting Elements in BcAMT Promoter Regions

To clarify transcriptional regulation of *BcAMT*, 2,000 bp upstream promoter regions were used to analyze *cis*-acting elements using PlantCARE database. 42 types of elements were detected and grouped into four functional categories. (1) Light-responsive elements: 14 light-related regulatory motifs, including G-Box, GT1-motif, and TCT-motif, were detected in most *BcAMT* promoters. (2) Growth- and development-related elements: AAGAA-motif, O_2-site, and CAT-box motifs were present in *BcAMT* promoters, while circadian element was identified exclusively in the promoters of *BcAMT1.1* and *BcAMT1.4*. (3) Hormone-response elements: Promoters contained binding sites responsive to gibberellin (GARE-motif, TATC-box, P-box), auxin (AuxRR-core, TGA-element),

 doi:10.20944/preprints202511.1072.v1

abscisic acid (ABRE), salicylic acid (TCA-element), methyl jasmonate (CGTCA-motif), and ethylene (ERE). Notably, ABRE, ERE, and CGTCA-motif were widely distributed among promoters. (4) Stress-related elements: 13 types of stress-related motifs were detected, including stress-responsiveness element (STRE), anaerobic induction element (ARE), salicylic acid or pathogen-induced signaling (as-1), low-temperature responsiveness (LTR), wound-responsive element (WUN-motif), and several MYB/ MYC- binding sites (Figure 5). These findings indicate that *BcAMT*s transcription may be regulated by various environmental and endogenous factors, including light, hormonal signaling, growth and development, and abiotic or biotic stresses.

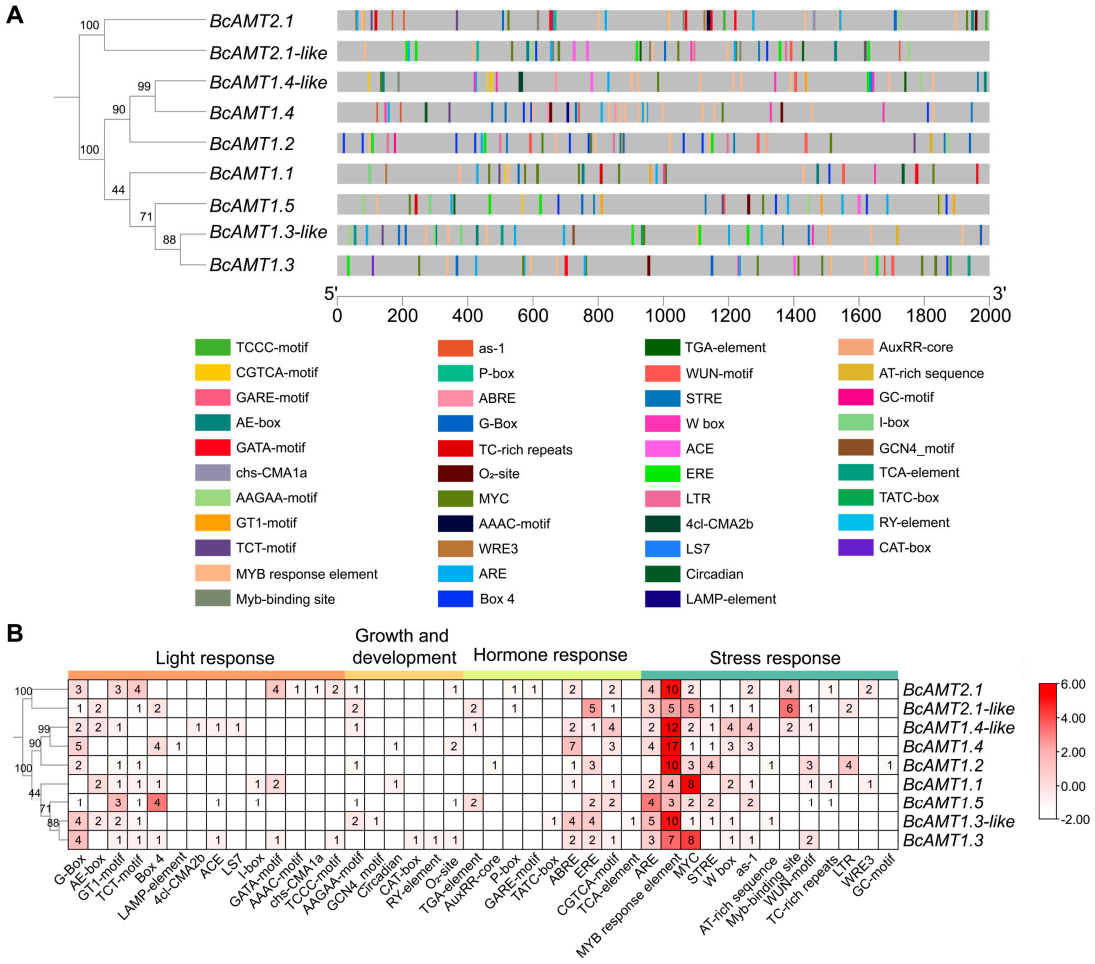

Figure 5. Analysis of *cis*-acting elements in *BcAMTs* promoters. (**A**) Distribution of cis-acting elements. (**B**) Number of each cis-acting element type.

2.6. Expression Patterns of BcAMTs Across Tissues of Flowering Chinese Cabbage and Under Different Nitrogen Forms

2.6.1. Tissue-Specific Expression

The data of RNA-sequencing (RNA-seq) from the cultivar '49 Caixin'(SRP427920) revealed distinct spatial expression patterns for *BcAMTs* in seven tissues (roots, stems, flowers, seedpods, and young/mature/senescent leaves). *BcAMT1.1*, *BcAMT2.1*, and *BcAMT2.1-like* were broadly expressed in tissues, with *BcAMT1.1* showing high transcript abundance in leaves, stems, and roots; *BcAMT2.1* in young/mature leaves, seedpods, stems and roots; and *BcAMT2.1-like* in young/mature leaves, and stems (Figure 6A). *BcAMT1.2* was strongly expressed in roots and stems, *BcAMT1.3* and *BAMT1.5* were specifically high expressed in roots, *BcAMT1.4* and *BcAMT1.4-like* were specifically expressed in flowers, while *BcAMT1.3-like* exhibited low expression in most tissues (Figure 6A). The results

 doi:10.20944/preprints202511.1072.v1

indicate that *BcAMTs* may play distinct roles in regulating plant growth and development of flowering Chinese cabbage.

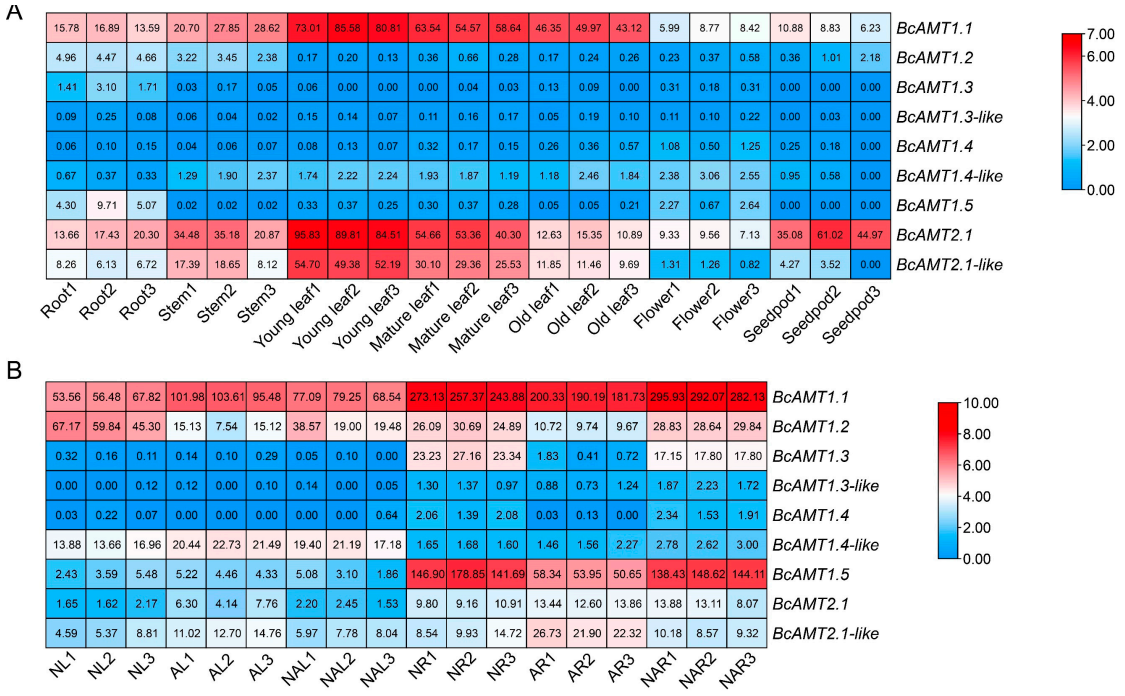

Figure 6. Expression characteristics of *BcAMTs* in flowering Chinese cabbage. (**A**) Expression in different tissues. (**B**) Expression under different nitrogen regimes. AL and AR: leaf and root in 1 mmol·L^{-1} NH_4^+; NAL and NAR: leaf and root in 0.5 mmol·L^{-1} NH_4^+ and 0.5 mmol·L^{-1} NO_3^-; NL and NR: leaf and root in 1 mmol·L^{-1} NO_3^-. Heatmap represents normalized FPKM and values in rectangle represent raw data.

2.6.2. BcAMTs Response to Nitrogen Forms

Expression changes were evaluated following treatments with different nitrogen sources: 1 mmol·L^{-1} NH_4^+, 0.5 mmol·L^{-1} NH_4^+ and 0.5 mmol·L^{-1} NO_3^-, and 1 mmol·L^{-1} NO_3^- for 4 d (PRJCA021671). The transcripts of *BcAMT1.1* were abundant in both leaves and roots in response to different nitrogen sources. In leaves, *BcAMT1.1* transcription was significantly up-regulated under both NH_4^+ and the mixed nitrogen nutrition compared with NO_3^- treatment; in roots, its expression was reduced by NH_4^+ but increased under the mixed treatment (Figure 6B). The transcription of *BcAMT1.3* and *BcAMT1.5* in leaves was unaffected by nitrogen forms; while in roots, the ones were significantly decreased by NH_4^+ and only slightly altered by the mixed nitrogen treatment (Figure 6B). In contrast, the transcripts of *BcAMT2.1* and *BcAMT2.1-like* were strongly induced by NH_4^+ and the mixed nitrogen nutrition in both roots or leaves, compared with the ones of NO_3^- (Figure 6B). These results show that the BcAMT gene exhibited a dynamic response to various nitrogen treatments, suggesting that it may play a key role in nitrogen uptake and metabolism.

2.6.3. Response to Nitrogen Deficiency and Different NH_4^+ Concentration

The qRT-PCR analysis revealed that *BcAMT1.1* transcript was markedly induced under nitrogen deficiency. After 72 h of nitrogen starvation, *BcAMT1.1* expression increased 6.78-fold in roots and 2.01-fold in leaves compared with the control (Figure 7A, B). When exposed to different NH_4^+ concentrations, *BcAMT1.1* transcripts were significantly up-regulated by lower NH_4^+ levels, reaching 1.95 ~ 4.10 times that of the control. In contrast, the ones were obviously down-regulated by higher NH_4^+ concentration, only being 1.25 ~ 1.73 times of the control (Figure 7C, D). Considering the established role of AMT1 subfamily members in high-affinity NH_4^+ uptake, their inducibility under nitrogen deficiency or low nitrogen conditions, *BcAMT1.1* was selected for subsequent functional characterization.

 doi:10.20944/preprints202511.1072.v1

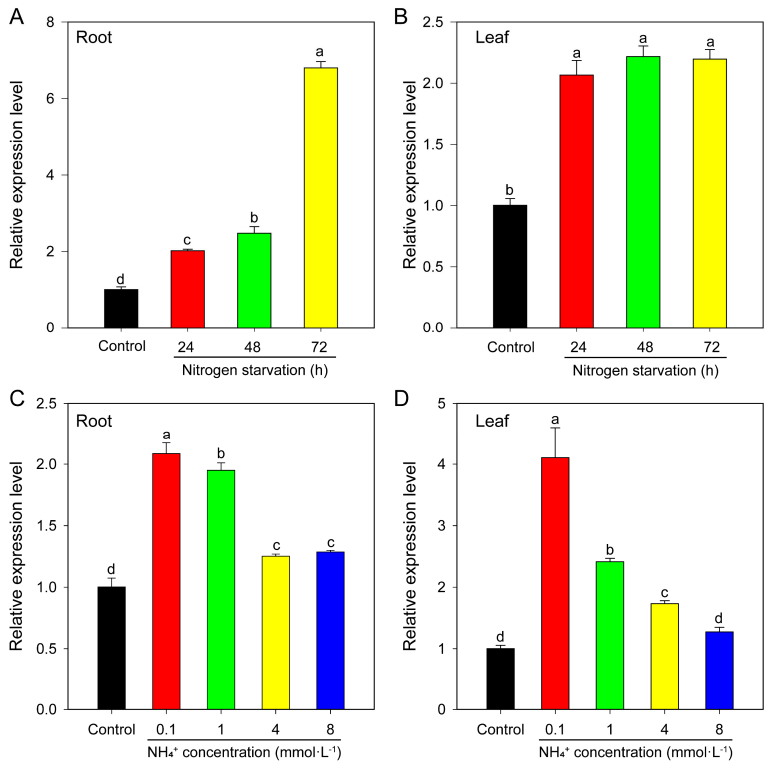

Figure 7. *BcAMT1.1* expression patterns in flowering Chinese cabbage determined by qRT-PCR under different nitrogen regimes. After cultivation for two weeks at 4 mmol·L^{-1} NO_3^-, seedlings of flowering Chinese cabbage were subjected to different nitrogen treatments. (**A, B**) *BcAMT1.1* expression in roots and leaves under nitrogen deficiency for 0, 24, 48, and 72 h. (**C, D**) *BcAMT1.1* expression in roots and leaves subjected to different NH_4^+ concentrations for 2 h. Different lowercase letters present the differences at the level of 0.05.

2.7. Subcellular Localization and NH_4^+ Transport Activity of BcAMT1.1

Transient expression assays indicated that BcAMT1.1 was localized in plasma membrane of onion epidermal cells (Figure 8A). NH_4^+ transport function of BcAMT1.1 was further examined using the yeast mutant 31019b. Transformants harboring pYES2-BcAMT1.1 grew normally on medium supplied with 2 mmol·L^{-1} NH_4^+ (Figure 8B). These findings indicate that BcAMT1.1 can complement the growth defect of the mutant, confirming its potential involvement in ammonium transport and utilization in yeast.

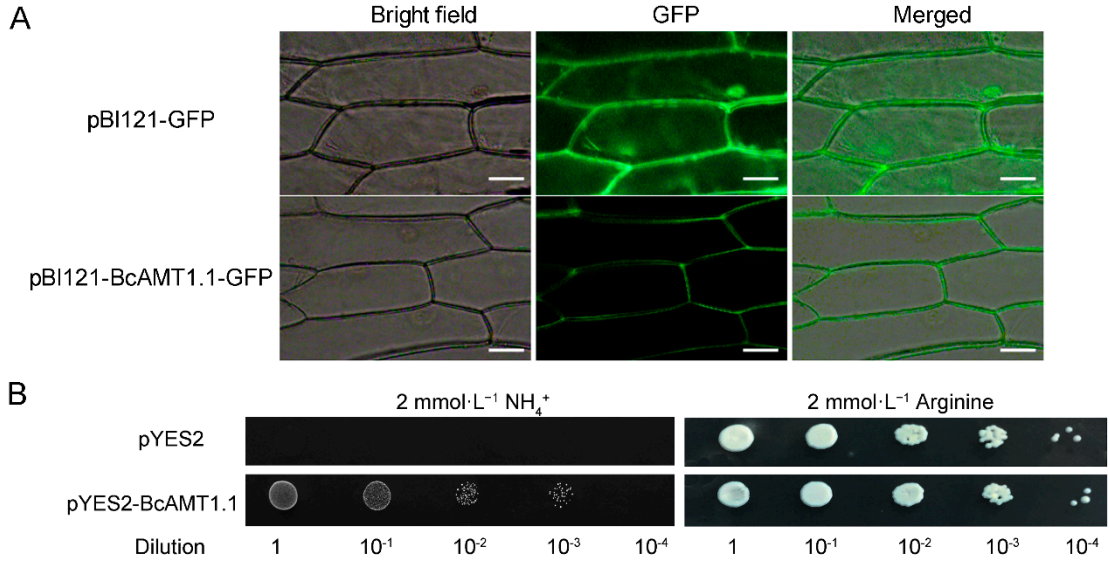

 doi:10.20944/preprints202511.1072.v1

Figure 8. Subcellular localization and NH_4^+ transport activity of BcAMT1.1. (**A**) Subcellular localization of BcAMT1.1. Scale bar is 50 μm. (**B**) Yeast complementation assay of BcAMT1.1 in mutant strain 31019b.

2.8. Overexpressing BcAMT1.1 Promotes NH_4^+ Uptake and Accelerates Plant Growth of Arabidopsis Under Low NH_4^+ Concentration

To evaluate the potential role of BcAMT1.1, three independent T_4 homozygous *Arabidopsis* lines were selected to analyze (Figure S1). After pre-cultivation on medium with 4 mmol·L^{-1} NO_3^- for 4 d, seedlings were subsequently transferred into vertical agar plates with 0.25 mmol·L^{-1} NH_4^+ for 10 d. Compared with wildtype (WT), overexpressing *BcAMT1.1* obviously promoted the growth of *Arabidopsis* seedlings, with shoots and roots fresh weight increased by 1.32 ~ 1.34 times and 2.04 ~ 2.36 times, respectively. Primary root length was increased by 1.10 ~ 1.16 folds (Figure 9A-C). NH_4^+ content in transgenic lines was 1.03 ~ 1.13 times higher than that of WT (Figure 9D). Net NH_4^+ influx rate was measured in the OE-2 line, was increased by 20% relative of WT (Figure 9E).

The physiological relevance of this trait was confirmed by sensitivity testing with methylammonium (MeA), a toxic analog of NH_4^+. On medium with 20 mmol·L^{-1} MeA, overexpression lines showed severe growth inhibition, with fresh weight reduced by 35 ~ 48% of WT, accompanied by chlorosis and shorter primary roots (Figure S2). Collectively, these results demonstrate that overexpressing *BcAMT1.1* enhances NH_4^+ uptake capacity under low NH_4^+ conditions, and promotes plant growth.

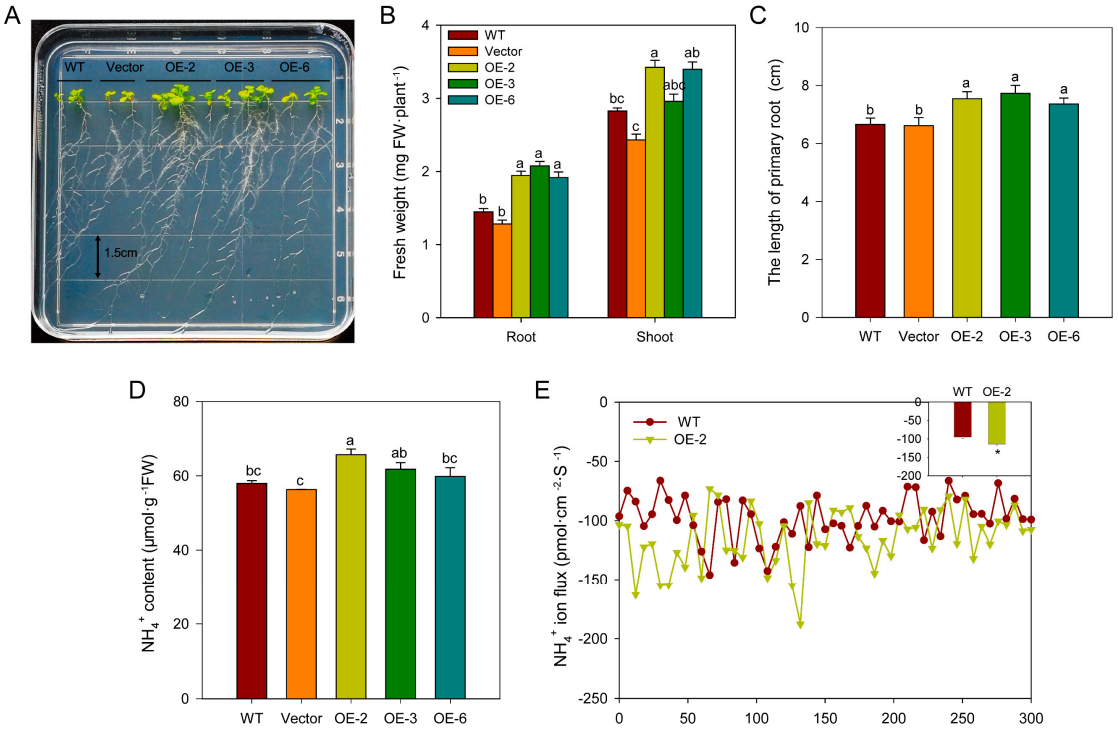

Figure 9. Phenotype and physiological traits of *BcAMT1.1*-overexpressing *Arabidopsis* under 0.25 mmol·L^{-1} NH_4^+. (**A**) Growth phenotype of wild type (WT), vector control and overexpressing *BcAMT1.1* lines. After precultured on solid medium contained 4 mmol·L^{-1} NO_3^- for 4 d, seedlings were transferred to 0.25 mmol·L^{-1} NH_4^+ for 10 d. (**B**) Fresh weight of whole pants. (**C**) Primary root length. (**D**) NH_4^+ content of whole plants. (**E**) NH_4^+ ion flux in root surface. WT: wild type; vector: overexpressing pCAMBIA 3301 vector; OE-2, OE-3, an OE-6: overexpression lines 2, 3, and 6. Line chart shows the real-time change of NH_4^+ ion at root surface during 5 min; small histogram presents net NH_4^+ change. Lowercase letters or asterisks denote significant difference ($P < 0.05$).

2.9. Overexpressing BcAMT1.1 Alters Nitrogen Ion Fluxes and the Expression of Nitrogen Assimilation-Related Genes in Arabidopsis

 doi:10.20944/preprints202511.1072.v1

To further explore the function of BcAMT1.1, the OE-2 line was used to detect the function under a nitrogen mixed nutrition (0.0625 mmol·L^{-1} NH_4^+ and 0.1875 mmol·L^{-1} NO_3^-). Overexpressing *BcAMT1.1* lines exhibited better growth potential than WT, characterized by significantly increased biomass, elongated primary root length, increased lateral roots number and density (Figure 10A-D). Net NH_4^+ influx in OE-2 was 1.74-fold higher than in WT, whereas NO_3^- flux shifted from net influx in WT to net efflux in OE-2 (Figure 10E). NO_3^- content was significantly decreased in transgenic seedlings, whereas NH_4^+ content remained unchanged (Figure 10F).

Furthermore, we detected the transcript level of key nitrogen assimilation-related genes, such as *GLN*, *GLT*, and *GDH*, encoding GS, GOGAT, and glutamate dehydrogenase. Transcript analysis of nitrogen assimilation-related genes revealed that overexpressing *BcAMT1.1* significantly up-regulated *AtGLN1;2* transcription, being about 2.60 folds of WT, and significantly down-regulated the expression of *AtGLN2* in roots; while having no obvious influences on *AtGLN1.1*, *AtGDH2*, and *AtGLT1* (Figure 10G). In shoots, the transcription of *AtGLN1.1*, *AtGLN2*, and *AtGDH2* in overexpression lines were significantly improved by 2.08, 2.16, and 7.31 times, respectively, compared to those of WT (Figure 10H).

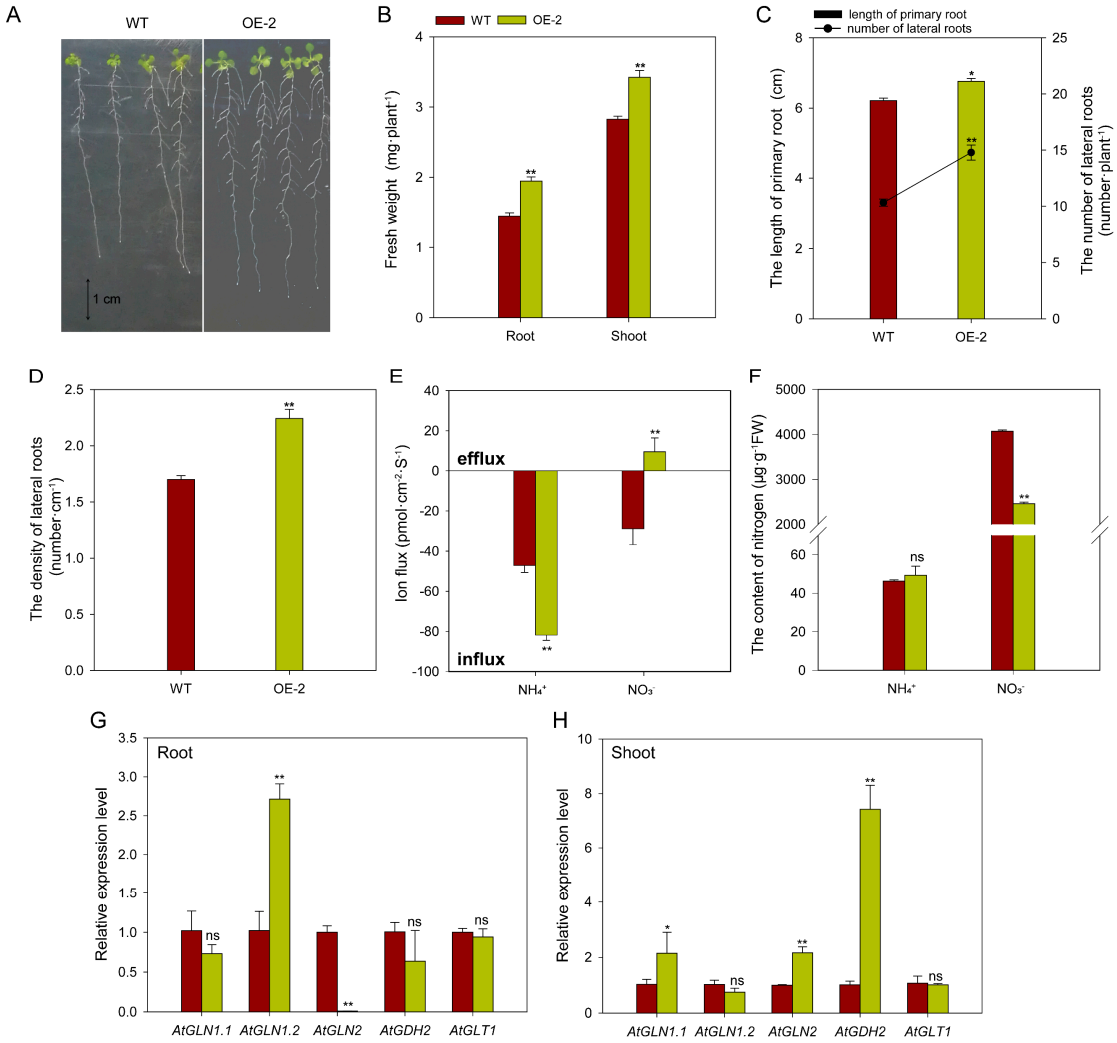

Figure 10. Effect of Overexpressing *BcAMT1.1* on plant growth, nitrogen uptake, and assimilation under mixed NH_4^+ and NO_3^- nutrition. (**A**) Plant phenotype. (**B**) Fresh weight of roots and shoots. (**C**) Primary root length and lateral roots numbers. (**D**) Lateral roots density. (**E**) NH_4^+ and NO_3^- ion fluxes. (**F**) NH_4^+ and NO_3^- content. (**G**, **H**) Expression of nitrogen assimilation-related genes in roots and shoots. WT: wild type; OE-2: overexpression line 2. ns: no significant difference; * or ** represents significant differences at $P < 0.05$ or $P < 0.01$, respectively.

2.10. Protein-Protein Interaction (PPI) Network of BcAMT1.1

 doi:10.20944/preprints202511.1072.v1

To further elucidate the potential molecular mechanism of BcAMT1.1, a PPI network was inferred from orthologous genes in *Arabidopsis* using the STRING database. The analysis identified 46 putative interaction pairs (Figure 11; Table S3). In this network, BcAMT1.1 was predicted to interact with AMT1.3, nitrate transporter (NPF6.3/NRT1.1, NRT2.1 and NRT2.4), GLT1.1, GLN (GLN1.3, GLN1.4, and GLN2), and GLB1, which is a PII protein involved in nitrogen-sensing signal transduction pathway [31]. In addition, BcAMT1.1 may interact with CBL-interacting protein kinase 23 (CIPK23), which forms a complex with the calcineurin B-like protein (CBL), who play a prominent role in activation on plant nutrient transporter [32]. Notably, CIPK23 was also predicted to interact with AMT1.3, NRT2.1, NRT2.4, and NPF6.3. The observations suggest that AMT1.1 may participate in nitrogen absorption and assimilation through interactions with CIPK23 and other key regulators within nitrogen metabolism network.

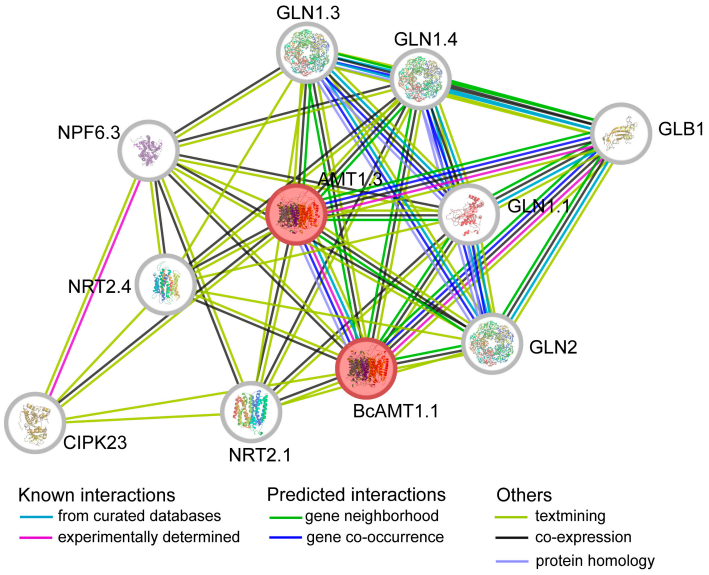

Figure 11. Predicted protein-protein interaction network of BcAMT1.1.

3. Discussion

AMT proteins are key mediators of NH_4^+ absorption and transport from rhizosphere to intercellular space, thereby maintaining cellular NH_4^+ homeostasis [14,33]. Although the *AMT* gene families have been well characterized in a variety of species, such as *Arabidopsis*, *O. sativa*, and *B. napus*, a comprehensive and systematic identification in flowering Chinese cabbage remains lacking. In this study, nine *BcAMT* genes were systematically identified and categorized into two phylogenetic subfamilies: AMT1 (7 members) and AMT2 (2 members), consistent with the classification of AtAMTs in *Arabidopsis* and BnaAMTs in *B. napus* (Figure 2). Interestingly, while each *Arabidopsis* AMT has a single homologous copy, most *B. napus* AMTs occur as 2 ~ 3 copies. In flowering Chinese cabbage, BcAMT1.1, BcAMT1.2 and BcAMT1.5 existed as a single copy, BcAMT1.3, BcAMT1.4 and BcAMT2.1 contained two copies. These homologous genes clustered into the corresponding branches with AMT proteins from other species (Figure 2), consistent with the higher number of duplicated orthologs in *Brassica* species than *Arabidopsis* [34], supporting previous evidence for higher levels of duplicated orthologs in *Brassica* compared with *Arabidopsis*. Previous study has reported that three polyploidization events in *B. rapa*: γ triplication (135 MYA), β duplication (90 ~ 100 MYA), and α duplication (24 ~ 40 MYA) [35]. In our study, five of nine *BcAMT* genes (55.56%) were products of segmental duplication (Figure 4; Table 2), suggesting that the expansion of *BcAMTs* in flowering Chinese cabbage was primarily driven by segmental duplication.

Polyploidization often leads to the diversification in both structural features and functional domains of genes. In this study, motif analysis revealed that BcAMT1 subfamily members in

 doi:10.20944/preprints202511.1072.v1

flowering Chinese cabbage possessed 10 uniform motifs, whereas BcAMT2 members lacked motif 1, motif 2, and motif 9, with BcAMT2.1-like further lacking motif 7 (Figure 3). Similar reductions of conserved motif number in AMT2 subfamily compared with AMT1 have been reported in *B. napus* [19]. Previous studies have reported that most *AMT1* genes lack introns, with exception including *LjAMT1.1* in *Lotus japonicus* [36], *SlAMT1.2* in *Solanum lycopersicum* [37], and *MeAMT1.2* in *Manihot esculenta* [38]. In this study, both *BcAMT1.2* and *BcAMT1.3-like* contained one intron, with the intron length of *BcAMT1.3-like* exceeding 4500 bp (Figure 3). A similarly long intron structure is found in rapeseed *BnaAMT1.3a* [19]. All *BcAMT2* genes contained four introns and five exons, being consistent with those reported in *Arabidopsis* [33], *B. napus* [19], and soybean [20]. It indicates that these *AMT2* genes may undergo more complex regulation, i.e., chromatin assembly, mRNA transport, and alternative splicing [39].

In plants, the members of AMT1 subfamily are widely recognized as high-affinity ammonium transporters [11,22], whereas AMT2 members are primarily associated with low-affinity transport [33]. In flowering Chinese cabbage, *BcAMTs* exhibits distinct expression profiles. *BcAMT1.5* is predominantly expressed in roots [40]. In this study, RNA-seq analysis revealed that *BcAMT1.1*, *BcAMT2.1*, and *BcAMT2.1-like* were mainly expressed in roots, stems, and leaves. Notably, *BcAMT1.1* was strongly induced under nitrogen-deficient or low nitrogen availability, particularly in roots (Figure 7). It is consistent with previous studies that *AtAMT1.1* in *Arabidopsis* [41], *OsAMT1.1* in *O. sativa* [18], and *PsAMT1.1* in *Populus simonii* [42] are induced under limited nitrogen availability and function as high-affinity ammonium transporters.

In the present study, BcAMT1.1 was located at the plasma membrane and was able to complement the growth defect of yeast mutant 31019b on medium containing 2 mmol·L^{-1} NH_4^+. In *Arabidopsis*, overexpressing *BcAMT1.1* significantly promoted plant growth in low nitrogen conditions, being increased both net NH_4^+ influx and NH_4^+ content in comparison with the ones of WT. It indicates that *BcAMT1.1* encodes a high-affinity ammonium transporter in flowering Chinese cabbage. It is consistent with previous reports for AMT1.1 in *Arabidopsis* [22,41], *Oryza sativa* [18,43], and *P. simonii* [42], as well as with the results of BcAMT1.2 and BcAMT1.5 in *B. campestris*, which indicate that AMT1 members primarily function in NH_4^+ absorption and their overexpression lines can enhance NH_4^+ absorption at low NH_4^+ conditions. Under the mixed nitrogen nutrition, *BcAMT1.1*-overexpressing lines enhanced transcription of *AtGLN1.1*, *AtGLN1.2*, *AtGLN2*, *AtGDH2*, the key genes of GS/GOGAT or GDH pathway, leading to increasing net NH_4^+ influx without significant changes in NH_4^+ content in comparison to WT. This is in accordance with our earlier observations, which showed that overexpressing *BcAMT1.2* or *BcAMT1.5* significantly enhanced the transcription of most nitrogen assimilation-related genes[40,44]. Previous study has further indicated that potential NH_4^+ toxicity can be mitigated if nitrogen assimilation rates keep pace with the ones of NH_4^+ uptake [45].

Beyond their role in NH_4^+ absorption, AMTs may also affect NO_3^- uptake, owing to that the acquisition of these two nitrogen sources can be synergistically regulated [4]. Our results showed that in *BcAMT1.1*-overexpressing lines, net NO_3^- flux shifted from influx in WT to efflux, leading to a marked decrease in NO_3^- concentration. It aligns with the observations for *BcAMT1.2* in flowering Chinese cabbage [44], while contrasts with the results for *PsAMT1.1* in *P. simonii* [42] and *BcAMT1.5* in flowering Chinese cabbage [40]. It indicates that AMT members may have divergent functions in modulating the interaction between NH_4^+ and NO_3^- uptake [44].

AMTs activities are tightly regulated to adapt to external nitrogen status, with control exerted at both transcriptional and post-transcriptional levels [46–48]. Plant nutrient uptake, including both NO_3^- and NH_4^+, is often modulated by protein kinase-mediated phosphorylation at post-transcriptional levels [49]. For instance, CIPK23 regulates NO_3^- uptake by phosphorylating of a threonine in NPF6.3/NRT1.1 [32,50,51]. Similarly, conserved threonine residues in AtAMT1.1 and AtAMT1.2 are targeted for phosphorylation by the CBL1-CIPK23 complex [32,47,49]. In *Arabidopsis*, phosphorylation of threonine residues T464 and T494 in AtAMT1.3 serves as a key regulatory switch, enabling plant to fine-tune its response to varying nitrogen forms. [48]. In the present study, PPI

 doi:10.20944/preprints202511.1072.v1

network indicated that BcAMT1.1 might interact with CIPK23, as well as with other proteins involved in nitrogen uptake and metabolism, including AMT, NRT, GLT, GLN, and GLB proteins (Figure 11). These findings suggest that CIPK23 might contribute to regulating nitrogen uptake and assimilation by modifying phosphorylation residues on AMT, NRT, or other interacting proteins. Further identifying novel upstream regulators of AMT1s will be crucial for elucidating the molecular mechanisms of nitrogen transport [48].

4. Materials and Methods

4.1. Geonmoe-Wide Identification of AMT Genes in Flowering Chinese Cabbage and Chromosome Location

The genome database of flowering Chinese cabbage was obtained from the China National Gene Bank (CNGB) released by Li et al. [34]. Sequences of AtAMT in *Arabidopsis* were acquired from the *Brassicaceae* Database (BRAD) (http://brassicadb.cn/, accessed on 12 July 2024), and utilized as query inputs for BLASTP analysis against flowering Chinese cabbage genome (E-value < 1×10^{-5}). To confirm domain composition, candidate sequences were analyzed in the Pfam database (http://pfam.sanger.ac.uk/search, accessed on 12 July 2024) for the presence of the of ammonium transporter family domain (Pfam ID: PF00909). Phyicochemical properties of predicted AMT proteins were predicted using the ExPASY ProtParam (https://web.expasy.org/protparam/, accessed on 12 July 2024), and conserved domains were examined usng the NCBI Batch CD-Search tool (https://www.ncbi.nlm.nih.gov/Structure/bwrpsb/bwrpsb.cgi, accessed on 12 July 2024). Nine AMT proteins in flowering Chinese cabbage were finally confirmed as AMT family members. Predictions of subcellular localization were conducted with Deeploc-2.0 (https://services.healthtech.dtu.dk/cgi-bin/webface2.cgi, accessed on 12 July 2024), while transmembrane helices were identified with TMHMM v2.0 (https://services.healthtech.dtu.dk/services/TMHMM-2.0/, accessed on 12 July 2024). Chromosomal localization of *AMT* genes were analyzed and visualized using TBtools-II v2.345 [52].

4.2. Phylogenetic Tree, Conserved Motifs, Domains, and Gene Structure Analyses of AMT Members

Homologous AMT protein sequences from *A. thaliana*, *B. napus*, *S. lycopersicum*, *N. tabacum*, *O. sativa*, and *P. trichocarpa* were obtained from public database (BRAD, GenBank, UniProt, Genoscope) and literature [18,19,21,22]. A maximum-likelihood (ML) phylogenetic tree was generated based on the multiple sequence alignment of these seven species with 1000 bootstrap replicates, and visualized using Figtree v1.4.4. Sequences alignments were visualized and subfamily-specific conserved signature sequences were identified using Jalview v2.11.2.7 [53]. Conserved motifs of the flowering Chinese cabbage AMTs were performed using MEME Suite (https://meme-suite.org/meme/, assessed on 20 July, 2024), followed by analysis and visualization of domain organization and gene structures with TBtools-II.

4.3. Gene Duplication and Geneome-Wide Synteny Analysis of AMTs

Gene duplication events were analyzed and Ks and Ka parameters were calculated utilizing MCScan X module in TBtools-II. The diveragence rate (λ) was set to 1.5×10^{-8} for *B. rapa* [54], divergence time (T) was estimated as $T = Ks/2\lambda$, and the Ka/Ks ratio was calculated. Comparative synteny between flowering Chinese cabbage, *A. thaliana*, *B. napus*, and *O. sativa* was evaluated and visualized in TBtools-II.

4.4. Identification of Cis-Acting Elements in AMT Promoter Regions

The 2000 bp upstream sequences of *AMT* genes from flowering Chinese cabbage genome were obtained via TBtools-II, and cis-acting regulatory elements were identified using the PlantCARE database (https://bioinformatics.psb.ugent.be/webtools/ plantcare/html/, assessed on 23 August, 2024). Elements were classified according to functional categories, their distribution patterns were visualized using TBtools-II.

 doi:10.20944/preprints202511.1072.v1

4.5. Expression Profiling of BcAMTs

Expression levels of *BcAMT*s in different tissues (roots, stems, young leaves, mature leaves, old leaves, flowers, and seedpods) were retrieved from RNA-seq data (SRP427920) of flowering Chinese cabbage cultivar '49 Caixin'. Expression patterns under different nitrogen forms were obtained from unpublished RNA-seq datasets (PRJCA021671) of cultivar 'Youlv 501', After 4 d of nitrogen starvation, seedlings were treated with 1 mmol·L^{-1} NH_4^+, 0.5 mmol·L^{-1} NH_4^+ and 0.5 mmol·L^{-1} NO_3^-, and 1 mmol·L^{-1} NO_3^- for 4 d, the roots and leaves of which were collected for RNA sequencing. The values of fragments per kilobase of exon model per million mapped reads (FPKM) were utilized to generate heatmaps with TBtools-II.

Seedlings of flowering Chinese cabbage cultivar 'Youlv 501' at three-leaf stage were grown in a modified Hoagland solution with 4 mmol·L^{-1} NO_3^- for two weeks. Seedlings were rinsed thoroughly with deionized water and transplanted to a nitrogen-free modified Hoagland solution for nitrogen starvation. Leaves and roots were collected at 0, 24, 48, and 72 h after the initiation of nitrogen deprivation. The remaining seedlings were subsequently exposed to NH_4^+ at concentrations of 0.1, 1, 4, and 8 mmol·L^{-1} for 2 h, after which roots and leaves were harvested. Total RNA extraction, first-strand cDNA synthesis, and quantitative real-time PCR (RT-PCR) were conducted according to the method described by Zhu et al. [40].

4.6. Subcellular Localization of BcAMT1.1

Using primers listed in Table S4, the coding sequence (CDS) of *BcAMT1.1* without the termination codon was amplified and cloned into the pBI121-GFP vector after the vector was linearized by *Sma* I and *Xba* I. The BcAMT1.1-GFP plasmid was transformed into onion epidermal cells via *Agrobacterium tumefaciens* EHA105. GFP signals were observed using a Zeiss Axio Imager D2 fluorescence microscope.

4.7. Functional Complementation Analysis of BcAMT1.1 in Yeast

Using the ClonExpress II OneStep Cloning Kit (Vazyme Biotech, Nanjing, China), the *BcAMT1.1* CDS was inserted into the pYES2 vector, digested by *EcoR* I and *Xba* I. Recombinant plasmid and empty vector controls were transformed into yeast mutant strain 31019b (*Δmep1*, *Δmep2*, *Δmep3*, and *ura3*) via the method of lithium acetate. This strain is unable to grow on medium containing NH_4^+ concentration below 5 mmol·L^{-1} as the sole nitrogen source [22]. Transformants were cultured at 30 °C for 3 d on yeast nitrogen base medium (2% galactose) containing 2 mmol·L^{-1} arginine or NH_4^+ as the sole nitrogen source.

4.8. Overexpression of BcAMT1.1 in Arabidopsis

The *BcAMT1.1* CDS was cloned into pCAMBIA3301 and transformed into *Arabidopsis* via floral dip using *Agrobacterium tumefaciens* GV1301 [55]. Transgenic seeds were screened on phosphinothricin and analyzed by qRT-PCR. The T_4 generation homozygous lines were used to analyze plant phenotype and physicochemical indices.

Sterilized seeds were germinated on 1/2 Murashige and Skong (MS) agar medium containing 4 mmol·L^{-1} NO_3^- for 4 d, then transferred to 1/2 MS plates with 0.25 mmol·L^{-1} NH_4^+ for 10 d. Fresh weight, primary root length, and NH_4^+ content and NH_4^+ ion flux were measured as described by Zhu et al. [44].

For mixed nitrogen treatments, *Arabidopsis* seedlings were pre-cultured on 1/2 MS medium supplemented with 4 mmol·L^{-1} NO_3^- for 7 d, followed by transfer to 1/2 MS medium with 0.0625 mmol·L^{-1} NH_4^+ and 0.1875 mmol·L^{-1} NO_3^- for another 7 d. NH_4^+ and NO_3^- contents were determined following Ivančič and Degobbis [56]. Gene expression were analyzed via qRT-PCR using TB Green® Premix Ex Taq™ II (TaKaRa Bio, Shiga, Japan), with *GADPH* as the internal reference. Primers sequences were listed in Table S4. Relative transcript levels were evaluated using the $2^{-\Delta\Delta CT}$ method [57].

 doi:10.20944/preprints202511.1072.v1

4.9. Prediction of Protein-Protein Interaction Network of BcAMT1.1

A potential protein interaction partners of BcAMT1.1 was predicted using STRING database (https://cn.string-db.org, accessed on 25 August, 2024), with *Arabidopsis* orthologs used as reference.

4.10. Statistial Analysis

Statistical analyses were conducted using SPSS v21.0 (IBM, Armonk, NY, USA). Differenes among treatments were assessed by Duncan's multiple range test, with significance defined at $P < 0.05$ or $P < 0.01$. In the firgures, distinct lowercase letters or asterisks denote statistically significant differences among treatments.

5. Conclusions

This study presents a comprehensive characterization of the ammonium transporter (AMT) gene family in flowering Chinese cabbage, with emphasis on BcAMT1.1, a plasm membrane-localized isoform. Nine *BcAMT* genes were identified and categorized into two subgroups according to phylogenetic relationships and conserved domains. Expression profiles revealed that *BcAMT1.1* was preferentially expressed in roots, leaves, and stems, and displayed differential transcriptional responses to different nitrogen sources. Notably, *BcAMT1.1* was strongly induced under nitrogen starvation or low NH_4^+ levels, but markedly suppressed at higher NH_4^+ level. Functional assays demonstrated that overexpressing *BcAMT1.1* in *Arabidopsis* accelerated plant growth under low-nitrogen conditions, increased NH_4^+ influx, and content, and altered the expression of nitrogen assimilation-related genes compared with WT. Drawing upon these results, we propose a mechanistic model outlining how BcAMT1.1 regulates nitrogen uptake and assimilation (Figure 12). Collectively, these findings advance our understanding of AMT functions in flowering Chinese cabbage, and provide molecular insights for AMT-mediated regulation of nitrogen uptake and assimilation.

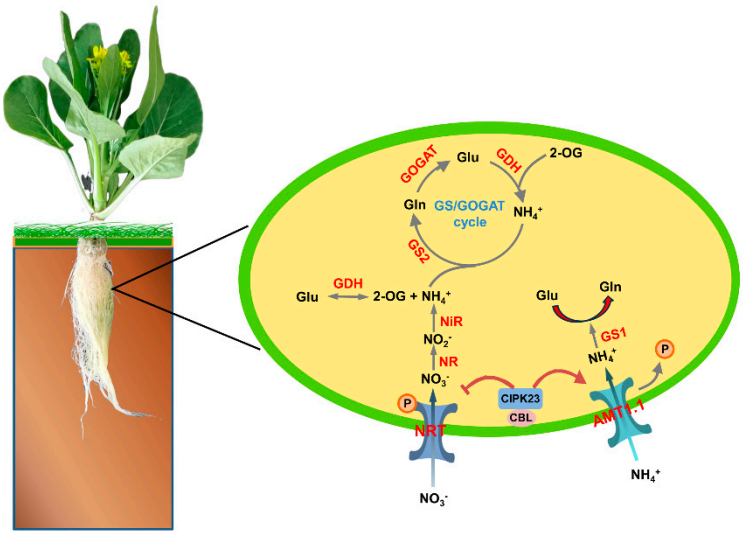

Figure 12. A proposed model for BcAMT1.1 regulates nitrogen uptake and assimilation under low NH_4^+ conditions.

Supplementary Materials: The following supporting information can be downloaded at: https://www.mdpi.com/article/doi/s1, Table S1. The sequence information for each AMT protein used for the phylogenetic analysis; Table S2. All gene pairs of three different genomes (*Brassica campestris* vs *Arabidopsis thaliana*, and *Brassica campestris* vs *Brassica napus*); Table S3: Protein-protein interaction network prediction of BcAMT1.1; Table S4: The primers were used in this study. Figure S1: Identification of qRT-PCR in different

 doi:10.20944/preprints202511.1072.v1

BcAMT1.1-overexpressing lines; Figure S2: Growth phenotype and fresh weight of overexpressing *BcAMT1.1* on NH_4^+ toxic analog methylammoium (MeA).

Author Contributions: R.C. and S. S. conceived and designed the project; Y.Z. and L.Z. performed the experiments; Y.Z., Q.Z. and X.H. analyzed the data, Y.Z. and L.Z. wrote the manuscript; A.A., W.S., and S.S. reviewed and edited the manuscript. All authors have read and agreed to the published version of the manuscript.

Funding: This research was funded by the National Natural Science Foundation of China (32202465), the Natural Science Foundation of Guangdong Province, China (2023A1515012687), the Guangdong Provincial Special Fund for Modern Agriculture Industry Technology Innovation Teams (2024CXTD01), and the China Agriculture Research System (CARS-23-B11).

Data Availability Statement: All datasets supporting this work are included within the article and Supplementary Materials.

Acknowledgements: We thank Bruno André from the Université Libre de Bruxelles for kindly providing the yeast mutant strain 31019b. We also thank the Guangxi First-class Disciplines (Agricultural Resources and Environment) for suggestions of this paper.

Conflicts of Interest: The authors declared no conflict of interest.

References

1. Kindred, D.R.; Verhoeven, T.M.O.; Weightman, R.M.; Swanston, J.S.; Agu, R.C.; Brosnan, J.M.; Sylvester-Bradley, R. Effects of variety and fertiliser nitrogen on alcohol yield, grain yield, starch and protein content, and protein composition of winter wheat. *J. Cereal. Sci.* **2008**, *48*, 46–57. https://doi.org/10.1016/j.jcs.2007.07.010.
2. Tei, F.; De Neve, S.; de Haan, J.; Kristensen, H.L. Nitrogen management of vegetable crops. *Agr. Water Manag*. **2020**, *240*, 106316. https://doi.org/10.1016/j.agwat.2020.106316.
3. Valenzuela, H. Optimizing the nitrogen use efficiency in vegetable crops. *Nitrogen* **2024**, *5*, 106–143. https://doi.org/10.3390/nitrogen5010008.
4. Xu, G.; Fan, X.; Miller, A.J. Plant nitrogen assimilation and use efficiency. *Annu. Rev. Plant Biol.* **2012**, *63*, 153–182. https://doi.org/10.1146/annurev-arplant-042811-105532.
5. Dechorgnat, J.; Nguyen, C.T.; Armengaud, P.; Jossier, M.; Diatloff, E.; Filleur, S.; Daniel-Vedele, F. From the soil to the seeds: the long journey of nitrate in plants. *J. Exp. Bot.* **2011**, *62*, 1349–1359. https://doi.org/10.1093/jxb/erq409.
6. Li, S.; Yan, L.; Zhang, W.; Yi, C.; Haider, S.; Wang, C.; Liu, Y.; Shi, L.; Ding, G. Nitrate alleviates ammonium toxicity in *Brassica napus* by coordinating rhizosphere and cell pH and ammonium assimilation. *Plant J.* **2024**, *117*, 786–804. https://doi.org/10.1111/tpj.16529.
7. Bloom, A.J.; Burger, M.; Asensio, J.S.R.; Cousins, A.B. Carbon dioxide enrichment inhibits nitrate assimilation in wheat and *Arabidopsis*. *Science* **2010**, *328*, 899–903. https://doi.org/10.1126/science.1186440.
8. Liu, X.; Hu, B.; Chu, C. Nitrogen assimilation in plants: current status and future prospects. *J. Genet. Genomics.* **2022**, *49*, 394–404. https://doi.org/10.1016/j.jgg.2021.12.006.
9. Omari Alzahrani, F. Ammonium transporter 1 (AMT1) gene family in pomegranate: genome-wide analysis and expression profiles in response to salt stress. *Curr. Issues. Mol. Biol.* **2025**, *47*, 59. https://doi.org/10.3390/cimb47010059.
10. Couturier, J.; Montanini, B.; Martin, F.; Brun, A.; Blaudez, D.; Chalot, M. The expanded family of ammonium transporters in the perennial poplar plant. *New. Phytol.* **2007**, *174*, 137–150. https://doi.org/10.1111/j.1469-8137.2007.01992.x.
11. Williamson, G.; Harris, T.; Bizior, A.; Hoskisson, P.A.; Pritchard, L.; Javelle A. Biological ammonium transporters: evolution and diversification. *FEBS J.* **2024**, *291*, 3786–3810. https://doi.org/10.1111/febs.17059.
12. Glass, A.D.M.; Britto, D.T.; Kaiser, B.N.; Kinghorn, J.R.; Kronzucker, H.J.; Kumar, A.; Okamoto, M.; Rawat, S.; Siddiqi, M.Y.; Unkles, S.E.; Vidmar, J.J. The regulation of nitrate and ammonium transport systems in plants. *J. Exp. Bot.* **2002**, *53*, 855–864. https://doi.org/10.1093/jexbot/ 53.370.855.

 doi:10.20944/preprints202511.1072.v1

13. McDonald, T.R.; Ward, J.M. Evolution of electrogenic ammonium transporters (AMTs). *Front. Plant Sci.* **2016**, *7*. https://doi.org/10.3389/fpls.2016.00352.
14. Ludewig, U.; Neuhäuser, B.; Dynowski, M. Molecular mechanisms of ammonium transport and accumulation in plants. *Febs. Lett.* **2007**, *581*, 2301–2308. https://doi.org/10.1016/j.febslet.2007.03. 034.
15. Sohlenkamp, C.; Shelden, M.; Howitt, S.; Udvardi, M. Characterization of *Arabidopsis* AtAMT2, a novel ammonium transporter in plants. *Febs. Lett.* **2000**, *467*, 273–278. https://doi.org/10.1016/ s0014-5793(00)01153-4.
16. Ninnemann, O.; Jauniaux, J.C.; Frommer, W.B. Identification of a high affinity NH_4^+ transporter from plants. *EMBO J.* **1994**, *13*, 3464–3471. https://doi.org/10.1002/j.1460-2075.1994.tb06652.x.
17. Li, B.; Merrick, M.; Li, S.; Li, H.; Zhu, S.; Shi, W.; Su, Y. Molecular basis and regulation of ammonium transporter in rice. *Rice Sci.* **2009**, *16*, 314–322. https://doi.org/10.1016/S1672-6308(08)60096-7.
18. Konishi, N.; Ma, J.F. Three polarly localized ammonium transporter 1 members are cooperatively responsible for ammonium uptake in rice under low ammonium condition. *New Phytol.* **2021**, *232*, 1778–1792. https://doi.org/10.1111/nph.17679.
19. Dai, J.; Han, P.; Walk, T.C.; Yang, L.; Chen, L.; Li, Y.; Gu, C.; Liao, X.; Qin, L. Genome-wide identification and characterization of ammonium transporter (AMT) genes in rapeseed (*Brassica napus* L.). *Genes* **2023**, *14*, 658. https://doi.org/10.3390/genes14030658.
20. Yang, W.; Dong, X.; Yuan, Z.; Li, X.; Wang, Y. Genome-wide identification and expression analysis of the ammonium transporter family genes in soybean. *Int. J. Mol. Sci.* **2023**, *24*, 3991. https://doi.org/10.3390/ijms24043991.
21. Liu, L.; Fan, T.; Shi, D.; Li, C.; He, M.; Chen, Y.; Zhang, L.; Yang, C.; Cheng, X.; Chen, X.; Li, D.; Sun Y. Coding-sequence identification and transcriptional profiling of nine AMTs and four NRTs from tobacco revealed their differential regulation by developmental stages, nitrogen nutrition, and photoperiod. *Front. Plant Sci.* **2018**, *9*, 210. https://doi.org/10.3389/fpls.2018.00210.
22. Yuan, L.; Loqué, D.; Kojima, S.; Rauch, S.; Ishiyama, K.; Inoue, E.; Takahashi, H.; von Wirén, N. The organization of high-affinity ammonium uptake in *Arabidopsis* roots depends on the spatial arrangement and biochemical properties of AMT1-type transporters. *Plant Cell* **2007**, *19*, 2636–2652. https://doi.org/10.1105/tpc.107.052134.
23. Sohlenkamp, C.; Wood, C.C.; Roeb, G.W.; Udvardi, M.K. Characterization of *Arabidopsis* AtAMT2, a high-affinity ammonium transporter of the plasma membrane. *Plant Physiol.* **2002**, *130*, 1788–1796. https://doi.org/10.1104/pp.008599.
24. Yuan, L.; Graff, L.; Loqué, D.; Kojima, S.; Tsuchiya Y.N.; Takahashi, H.; von Wirén, N. AtAMT1;4, a Pollen-specific high-affinity ammonium transporter of the plasma membrane in *Arabidopsis*. *Plant Cell Physiol.* **2009**, *50*, 13–25. https://doi.org/10.1093/pcp/pcn186.
25. Li, C.; Tang, Z.; Wei, J.; etc. The OsAMT1.1 gene functions in ammonium uptake and ammonium-potassium homeostasis over low and high ammonium concentration ranges. *J. Genet. Genomics* **2016**, *43*, 639–649. https://doi.org/10.1016/j.jgg.2016.11.001.
26. Zhao, Y.; Li, G.; Zhu, Z.; Hu., M.; Chen, M.; Wang, J.; Zhang, K.; Zheng, Y.; Liao, Y.; Chen C. Genomic selection and genetic architecture of agronomic traits during modern flowering Chinese cabbage breeding. *Hortic Res.* **2025**, *12*, uhae299. https://doi.org/10.1093/hr/uhae299.
27. Huang, X.; He, L.; Chen, Y.; Liu, Y.; Liu, J.; Chen, R.; Zhu., Y.; Song, S.; He, Q. Genome-wide identification of *SWEET* gene family and functional analysis of *BcSWEET1-2* associated with flowering in flowering Chinese cabbage (*Brassica campestris*). *BMC Genomics* **2025**, *26*, 605. https://doi.org/10.1186/s12864-025-11808-2.
28. Zhang, S.; Li, G.; Wang, Y.; Anwar, A.; He, B.; Zhang, J.; Chen, C.; Hao, Y.; Chen, R.; Song, S. Genome-wide identification of *BcGRF* genes in flowering Chinese cabbage and preliminary functional analysis of BcGRF8 in nitrogen metabolism. *Front. Plant Sci.* **2023**, *14*, 1144748. https://doi.org/10.3389/fpls.2023.1144748.
29. Zhu, Y.; Qi, B.; Hao, Y.; Liu, H.; Sun, G.; Chen, R.; Song, S. Appropriate NH_4^+/NO_3^- ratio triggers plant growth and nutrient uptake of flowering Chinese cabbage by optimizing the pH value of nutrient solution. *Front. Plant Sci.* **2021**, *12*, 656144. https://doi.org/10.3389/fpls.2021.656144.

30. Song, S.; Yi, L.; Zhu, Y.; Liu, H.; Sun, G.; Chen, R. Effects of ammonium and nitrate ratios on plant growth, nitrate concentration and nutrient uptake in flowering Chinese cabbage. *Bangl. J. Bot.* **2017**, *46*, 1259–1267.
31. Hsieh, M.H.; Lam, H.M.; van de Loo, F.J.; Coruzzi, G. A PII-like protein in Arabidopsis: putative role in nitrogen sensing. *PNAS* **1998**, *95*, 13965–13970. https://doi.org/10.1073/pnas.95.23.13965.
32. Ródenas, R.; Vert, G. Regulation of root nutrient transporters by CIPK23: 'One kinase to rule them all'. *Plant Cell Physiol.* **2021**, *62*, 553–563. https://doi.org/10.1093/pcp/pcaa156.
33. Giehl, R.; Laginha, A.M.; Duan, F.; Rentsch, D.; Yuan, L.; von Wirén, N. A critical role of AMT2;1 in root-to-shoot translocation of ammonium in *Arabidopsis*. *Mol. Plant.* **2017**, *10*, 1449–1460. https://doi.org/10.1016/j.molp.2017.10.001.
34. Li, G.; Jiang, D.; Wang, J.; Liao, Y.; Zhang, T.; Zhang, H.; Dai, X.; Ren, H.; Chen, C.; Zheng, Y. A high-continuity genome assembly of Chinese flowering cabbage (*Brassica rapa* var. *parachinensis*) provides new insights into *Brassica* genome structure evolution. *Plants* **2023**, *12*, 2498. https://doi.org/10.3390/plants12132498.
35. Wang, X.W.; Kole, C. The *Brassica rapa* genome. In *Compendium of Plant Genomes*, Chittaranjan, K.; Mohanpur, W.B. Eds. Springer-Verlag GmbH Berlin Heidelberg: Berlin, Germany, 2015; pp. 1–165. https://doi.org/101.1007/978-3-662-47901-8.
36. Salvemini, F.; Marini, A.; Riccio, A.; Patriarca, E.J.; Chiurazzi, M. Functional characterization of an ammonium transporter gene from *Lotus japonicus*. *Gene* **2001**, *270*, 237–243. https://doi.org/10.1016/S0378-1119(01)00470-X.
37. Filiz, E.; Akbudak, M.A. Ammonium transporter 1 (AMT1) gene family in tomato (*Solanum lycopersicum* L.) bioinformatics, physiological and expression analyses under drought and salt stresses. *Genomics* **2020**, *112*, 3773–3782. https://doi.org/10.1016/j.ygeno.2020.04.009.
38. Xia, Y.; Liu, Y.; Zhang, T.; Wang, Y.; Jiang, X.; Zhou, Y. Genome-wide identification and expression analysis of ammonium transporter 1 (AMT1) gene family in cassava (*Manihot esculenta* Crantz) and functional analysis of *MeAMT1;1* in transgenic *Arabidopsis*. *3 Biotech* **2022**, *12*, 4. https://doi.org/10.1007/s13205-021-03070-6.
39. Jo, B.; Choi, S.S. Introns: The Functional Benefits of Introns in Genomes. *Genomics Inform.* **2015**, *13*, 112. https://doi.org/10.5808/GI.2015.13.4.112.
40. Zhu, Y.; Zhong, L.; Huang, X.; Su, W.; Liu, H.; Sun, G.; Song., S.; Chen, R. *BcAMT1;5* mediates nitrogen uptake and assimilation in flowering Chinese cabbage and improves plant growth when overexpressed in *Arabidopsis*. *Horticulturae* **2023**, *9*, 43. https://doi.org/10.3390/horticulturae 9010043.
41. Gazzarrini, S.; Lejay, L.; Gojon, A.; Ninnemann, O.; Frommer, W.B.; von Wirén, N. Three functional transporters for constitutive, diurnally regulated, and starvation-induced uptake of ammonium into *Arabidopsis* roots. *Plant Cell* **1999**, *11*, 937–948. https://doi.org/10.1105/tpc.11.5. 937.
42. Zhang, C.; Chen, J.; Zhuang, S.; Feng, Z.; Fan, J. Functional characterization of PsAMT1.1 from Populus simonii in ammonium transport and its role in nitrogen uptake and metabolism. *Environ. Exp. Bot.* **2023**, *208*, 105255. https://doi.org/10.1016/j.envexpbot.2023.105255.
43. Ranathunge, K.; El-kereamy, A.; Gidda, S.; Bi, Y., Rothstein, S.J. AMT1;1 transgenic rice plants with enhanced NH_4^+ permeability show superior growth and higher yield under optimal and suboptimal NH_4^+ conditions. *J. Exp. Bot.* **2014**, *65*, 965–979. https://doi.org/10.1093/jxb/ert458.
44. Zhu, Y.; Huang, X.; Hao, Y.; Su, W.; Liu, H.; Sun, G.; Chen, R.; Song, S. Ammonium transporter (*BcAMT1.2*) mediates the interaction of ammonium and nitrate in *Brassica campestris*. *Front. Plant Sci.* **2020**, *10*, 1776. https://doi.org/10.3389/ fpls.2019.01776.
45. The, S.V.; Snyder, R.; Tegeder, M. Targeting nitrogen metabolism and transport processes to improve plant nitrogen use efficiency. *Front. Plant Sci.* **2021**, *11*, 628366. https://doi.org/10.3389/fpls.2020.628366.
46. Yuan, L.; Loqué, D.; Ye, F.; Frommer, W.B.; von Wirén, N. Nitrogen-dependent posttranscriptional regulation of the ammonium transporter AtAMT1;1. *Plant Physiol.* **2007**, *143*, 732–744. https://doi.org/10.1104/pp. 106.093237.
47. Straub, T.; Ludewig, U.; Neuhäuser, B. The kinase CIPK23 inhibits ammonium transport in *Arabidopsis thaliana*. *Plant Cell* **2017**, *29*, 409–422. https://doi.org/10.1105/tpc.16.00806.

 doi:10.20944/preprints202511.1072.v1

48. Wu, X.; Liu, T.; Zhang, Y.; Duan, F.; Neuhäuser, B.; Ludewig, U.; Schulze, W.X.; Yuan, L. Ammonium and nitrate regulate NH_4^+ uptake activity of Arabidopsis ammonium transporter AtAMT1;3 via phosphorylation at multiple C-terminal sites. *J. Exp. Bot.* **2019**, *70*, 4919–4930. https://doi.org/10.1093/jxb/erz230.
49. Wang, T.; Chen, X.; Ju, C.; Wang, C. Calcium signaling in plant mineral nutrition: From uptake to transport. *Plant Commun.* **2023**, *4*, 100678. https://doi.org/10.1016/j.xplc.2023.100678.
50. Wang, W.; Hu, B.; Li, A.; Chu, C. NRT1.1s in plants: functions beyond nitrate transport. *J. Exp. Bot.* **2020**, *71*, 4373–4379. https://doi.org/10.1093/jxb/erz554.
51. Ho, C.; Lin, S.; Hu, H.; Tsay, Y. CHL1 Functions as a Nitrate Sensor in Plants. *Cell* **2009**, *138*, 1184–1194. https://doi.org/10.1016/j.cell.2009.07.004.
52. Chen, C.; Wu, Y.; Li, J.; Wang, X.; Zeng, Z.; Xu, J.; Liu, Y.; Feng, J.; Chen, H.; He, Y.; Xia, R. TBtools-II: A "one for all, all for one" bioinformatics platform for biological big-data mining. *Mol. Plant* **2023**, *16*, 1733–1742. https://doi.org/10.1016/j.molp.2023.09.010.
53. Procter, J.B.; Carstairs, G.M.; Soares, B.; Mourão, K.; Ofoegbu, T.C.; Barton, D.; Lui, L.; Menard, A.; Sherstnev, N.; Roldan-Martinez, D.; Duce, S.; Martin, D.M.A.; Barton, G.J. Alignment of Biological Sequences with Jalview. In *Methods in Molecular Biology*, Katoh, K., Ed. Humana, New York, NY, 2021; Volume 2231, pp. 203–224. https://doi.org/10.1007/978-1-0716-1036-7_18.
54. Yin, X.; Wang, Q.; Chen, Q.; Xiang, N.; Yang, Y.; Yang, Y. Genome-wide identification and functional analysis of the calcineurin B-like protein and calcineurin B-like protein-interacting protein kinase gene families in turnip (*Brassica rapa* var. *rapa*). *Front. Plant Sci.* **2017**, *8*, 1191. https://doi.org/10.3389/fpls.2017.01191.
55. Wiktorek-Smagur, A.; Hnatuszko-Konka, K.; Kononowicz, A.K. Flower bud dipping or vacuum infiltration—two methods of *Arabidopsis thaliana* transformation. *Russ. J. Plant Physiol.* **2009**, *56*, 560–568. https://doi.org/10.1134/S1021443709040177.
56. Ivančič, I.; Degobbis, D. An optimal manual procedure for ammonia analysis in natural waters by the indophenol blue method. *Water Res.* **1984**, *18*, 1143–1147. https://doi.org/10.1016/0043-1354(84)90230-6.
57. Livak, K.J.; Schmittgen, T.D. Analysis of relative gene expression data using real-time quantitative PCR and the $2^{-\Delta\Delta CT}$ method. *Methods* **2001**, *25*, 402–408. https://doi.org/10.1006/ meth.2001.1262.